Urea-Induced Unfolding and Conformational Stability of 3-Isopropylmalate Dehydrogenase from the Thermophile *Thermus thermophilus* and Its Mesophilic Counterpart from *Escherichia coli*†

Chie Motono, Akihiko Yamagishi,* and Tairo Oshima

Department of Molecular Biology, Tokyo University of Pharmacy & Life Science, 1432 Horinouchi, Hachioji, Tokyo 192-0392, Japan

Received October 5, 1998; Revised Manuscript Received November 30, 1998

ABSTRACT: To reveal the basis of the thermal stability of 3-isopropylmalate dehydrogenase (IPMDH) from an extreme thermophile, *Thermus thermophilus*, urea-induced unfolding of the enzyme and of its mesophilic counterpart from *Escherichia coli* has been studied. The urea-induced equilibrium unfolding of *T. thermophilus* and *E. coli* IPMDHs at 27 °C was monitored by measuring the changes in far-UV CD, intrinsic fluorescence, anilinonaphthalenesulfonic acid (ANS) binding, and catalytic activity in the presence of nonionic detergent Tween 20. For both enzymes, the spectral methods revealed a biphasic unfolding transition. The first transition was protein concentration-independent, whereas the second was protein concentration-dependent for both enzymes. The observation suggested a three-state unfolding mechanism with a dimeric intermediate. However, the intermediates of the *E. coli* and the *T. thermophilus* IPMDHs seemed to be different from each other. The intermediate of the *E. coli* IPMDH lost its secondary and tertiary structure more than that of the thermophilic enzyme. *E. coli* IPMDH lost enzymatic activity through the transition from the native to the intermediate state, though the intermediate of the *T. thermophilus* enzyme was still active. The unfolding process of *E. coli* IPMDH can be explained by a sequential unfolding of individual folding domains, while there is only a small structural perturbation in the intermediate of *T. thermophilus* IPMDH. The higher thermal stability of *T. thermophilus* IPMDH can be attributed to the increase in the extent of interaction inside the first domain which unfolded prior to the unfolding of the whole molecular structure in *E. coli* IPMDH.

3-Isopropylmalate dehydrogenase (IPMDH, EC 1.1.1.85) is a bifunctional enzyme involved in the leucine biosynthesis pathway. It catalyzes the dehydrogenation and concomitant decarboxylation of the 3-isopropylmalate substrate, yielding 2-oxoisocaproate and carbon dioxide, using NAD^+ as a cofactor. The enzyme from an extreme thermophile, *Thermus thermophilus*, is a functional dimer composed of two identical subunits each with 345 amino acid residues (*1*). The polypepetide chain of a subunit is folded into two domains with similar folding topologies based on parallel α/β motifs (*2*).

IPMDH from *T. thermophilus*, which we will call *Tt*-IPMDH,[1] is 51% identical to the *Escherichia coli* enzyme (*Ec*-IPMDH) in terms of amino acid sequence (*3*). The temperatures of the native environment of the organisms are 37 and 75−80 °C for *E. coli* and *T. thermophilus*, respectively. They differ in their half-denaturation temperature: 63 and 83 °C for *Ec*-IPMDH and *Tt*-IPMDH, respectively. The two IPMDHs also differ in the level of enzyme activity, when measured at the same temperature (*4*). The structural comparison of *Tt*-IPMDH with their mesophilic counterparts from *E. coli* and *Salmonella typhimurium* has shown that main stabilizing features in the thermophilic enzyme are an increased number of salt bridges, additional hydrogen bonds, a proportionately larger and more hydrophobic subunit interface, shortened N and C termini, and a larger number of proline residues (*5*). It is, however, still unclear how these structural factors affect the thermostability or the unfolding of the IPMDH molecule. In this study, we compared the equilibrium unfolding process of the IPMDH from *T. thermophilus* with that of its counterpart from *E. coli*. We searched for equilibrium denaturation conditions and analyzed the urea-induced equilibrium unfolding of these IPMDHs.

EXPERIMENTAL PROCEDURES

Reagents. 3-Isopropylmalate (IPM) was purchased from Wako Pure Chemicals (Tokyo, Japan) and ultrapure urea from Nacalai tesque (Kyoto, Japan). All other reagents were of analytical grade. Water was purified by a Milli-Q purification system (Millipore).

Purification of IPMDH. Ec-IPMDH was overexpressed in *E. coli* BL21 harboring the plasmid pET21c, which carried the *leuB* gene of *E. coli*, then purified as described previously

† This work was supported by the Proposal-Based R&D Program of the New Energy and Industrial Technology Development Organization.

* To whom correspondence should be addressed: Department of Molecular Biology, Tokyo University of Pharmacy & Life Science, 1432 Horinouchi, Hachioji, Tokyo 192-0392, Japan. Telephone: +81-426-76-7139. Fax: +81-426-76-7145.

[1] Abbreviations: *Tt*-IPMDH, 3-isopropylmalate dehydrogenase from *T. thermophilus*; *Ec*-IPMDH, IPMDH from *E. coli*; IPM, 3-isopropylmalate; CD, circular dichroism; ANS, 1-anilinonaphthalene-8-sulfonic acid.

10.1021/bi982380v CCC: $18.00
Published on Web 01/05/1999

(*4*), and stored at 4 °C as a suspension in 60% saturated ammonium sulfate in potassium phosphate buffer. *Tt*-IPMDH was overexpressed and purified as described previously (*1*), and stored under the same conditions as *Ec*-IPMDH. The enzymes can be stored for several months without loss of activity under the conditions. The protein was collected by ultracentrifugation from the stock suspension, resolved in 50 mM potassium phosphate buffer (pH 7.0), and dialyzed against the same buffer at 4 °C prior to use. Protein concentrations were determined using a molar absorption coefficient of 30 400 at 280 nm (*1*). All concentrations of the IPMDH protein reported in this paper have units of molar (moles of monomer per liter). All samples and solutions were filtered through microporous filters (0.45 μm, Millipore) before use.

Protein Unfolding and Refolding Monitored by Intrinsic Fluorescence. Fluorescence measurements were taken with a Hitachi spectrofluorometer equipped with a thermostated cell holder. For equilibrium studies, *Ec*-IPMDH or *Tt*-IPMDH was incubated in 50 mM potassium phosphate (pH 7.0), 1 mM DTT, 0.01% Tween 20, and urea at 27 °C for 24 or 48 h, respectively. The fluorescence intensity was monitored at 340 and 332 nm for *Tt*-IPMDH and *Ec*-IPMDH, respectively (excitation at 280 nm), using 5 nm bandwidths on both sides with a quartz microcuvette with a 1 cm path length. All measurements were corrected for background signal of media containing the corresponding concentration of urea and repeated at least three times. For refolding experiments, *Ec*-IPMDH or *Tt*-IPMDH was denatured in the presence of 6 or 8 M urea, respectively, and then diluted 1:20 to lower urea concentrations so that the final protein concentration was 0.74 or 0.33 μM, respectively.

Unfolding Monitored by CD Spectroscopy. CD spectra were recorded with a JASCO J720 spectropolarimeter. Data were processed using software provided by JASCO on a NEC computer. Measurements were taken in a quartz cuvette with a 1 mm path length at 27 °C. Spectra were recorded as an average of six to eight scans from 250 to 215−200 nm for each sample. All measurements were repeated at least three times.

Enzyme Activity Assay. Enzyme activity was measured in 50 mM potassium phosphate buffer (pH 7.6) containing 0.1 M KCl, 0.2 mM $MnCl_2$, 1 mM NAD, and 0.5 mM IPM in a total volume of 500 μL, at 40 °C. The initial velocity was determined by monitoring the absorbance of NADH formed at 340 nm on a Beckman DU 7400 spectrophotometer. To prevent the refolding of unfolded proteins caused by dilution into the assay buffer, the assay buffer contained the same concentration of urea that was used for sample denaturation, in addition to the compounds listed above. At least three assays were performed.

ANS Binding Assay. Samples from urea denaturation series were assayed for hydrophobic surface exposure by incubation with a 50-fold molar excess of 1-anilinonaphthalene-8-sulfonic acid (ANS) for >60 min in the dark, followed by measuring the fluorescence emission spectra with excitation at 350 nm. Appropriate blank spectra of ANS in the corresponding denaturation buffers were subtracted to obtain the net fluorescence enhancement due to ANS binding to the protein. The concentration of ANS was determined using an extinction coefficient of 4.95×10^3 M^{-1} cm^{-1} at 350 nm in water.

Data Analysis. Experimental data could not be reconciled with a two-state mechanism. We therefore employed a three-state treatment. A dimeric intermediate was assumed to be in equilibrium with the native dimeric enzyme and unfolded subunits as will be described in the Discussion.

$$N_2 \overset{K_1}{\rightleftharpoons} I_2 \overset{K_2}{\rightleftharpoons} D + D \quad (1)$$

K_1 and K_2 are equilibrium constants related to the respective unfolding steps. The free energy change for each unfolding step is assumed to be linearly dependent on denaturant concentration as described by Pace et al. (*6*).

$$\Delta G_1 = \Delta G_1^\circ - m_1[\text{urea}] \quad (2)$$

$$\Delta G_2 = \Delta G_2^\circ - m_2[\text{urea}] \quad (3)$$

where ΔG_1° and ΔG_2° are the free energy changes in the absence of urea corresponding to equilibrium constants K_1 and K_2, respectively, and m_1 and m_2 are the cooperativity indices associated with the respective steps. The amplitude of the measured spectroscopic signal Y (intrinsic fluorescence intensity and CD at 222 nm) was assumed to be a linear combination of the fractional contribution from each species.

$$Y = Y_N f_N + Y_I f_I + Y_D f_D \quad (4)$$

where Y_N, Y_I, and Y_D are amplitudes of the signals for the respective species and f_N, f_I, and f_D are mole fractions in the native state, the intermediate state, and the unfolded state, respectively. f_N, f_I, and f_D are related to the equilibrium constants K_1 and K_2 as described by Clark et al. (*7*). A nonlinear least-squares fit of eq 4 to the spectroscopic data was used to estimate the fundamental parameters (ΔG_1°, ΔG_2°, m_1, m_2, and Y_I). Initial values for these parameters were calculated assuming that each unfolding step is a simple two-state transition.

RESULTS

Equilibrium Unfolding Processes of IPMDHs from E. coli and T. thermophilus by Urea. The spectral changes associated with the unfolding of IPMDH were studied by intrinsic fluorescence and circular dichroism at 222 nm. To reach the unfolding equilibrium at each urea concentration, all measurements were performed after incubation of the protein solution for 24 (*Ec*-IPMDH) or 48 h (*Tt*-IPMDH) at 27 °C. Clark et al. have reported that a low concentration of nonionic detergent, Tween 20, had the effect of improving the reversibility of bacterial luciferase and that Tween 20 affected little the stability of the enzyme (*7*). We also tested the refolding of the IPMDHs in the presence of Tween 20, and found that maximum refolding was obtained in the presence of 0.01% Tween 20. When *Ec*-IPMDH or *Tt*-IPMDH denatured in the presence of 6 or 8 M urea, respectively, was diluted 1:20 with the buffer without urea, the refolding yield measured by fluorescence or CD was more than 85% in the presence of Tween 20. Only 50−60% refolding was obtained in the absence of the detergent. Urea-induced unfolding in the absence of the detergent monitored by fluorescence showed a complex time course and did not attain equilibrium even after prolonged incubation (data not shown). We therefore could not estimate the reliable signal

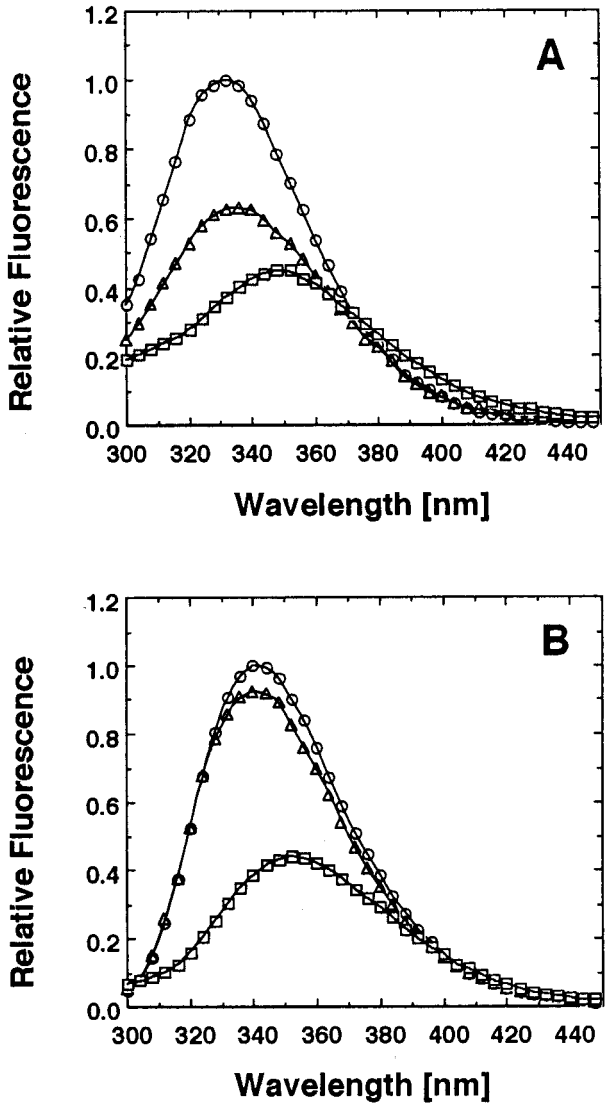

FIGURE 1: Fluorescence emission spectra of *Ec*-IPMDH and *Tt*-IPMDH. Fluorescence was excited at 280 nm. (A) *Ec*-IPMDH samples were incubated with either 0 (○), 3 (△), or 6 M (□) urea at 27 °C for 24 h. (B) *Tt*-IPMDH samples were incubated with either 0 (○), 4 (△), or 8 M (□) urea at 27 °C for 48 h.

amplitude of unfolding without the detergent. Accordingly, all of the following experiments were carried out in the presence of 0.01% Tween 20. Because precipitation was observed in renaturation experiments with protein concentrations of >3.3 μM, a concentration of <3.0 μM was used.

Panels A and B of Figure 1 show the fluorescence emission spectra of native, intermediate, and unfolded states of *Ec*-IPMDH and *Tt*-IPMDH, respectively. Native *Ec*-IPMDH and *Tt*-IPMDH had fluorescence emission maximum at about 332 and 340 nm, respectively, when excited at 280 nm. The fluorescence intensity of *Ec*-IPMDH decreased to 60%, which was accompanied by a red shift from 332 to 336 nm in the presence of 3 M urea. In the presence of 6 M urea, the fluorescence intensity decreased to 40% and the emission maximum shifted to 348 nm. The emission maximum of *Tt*-IPMDH did not shift in the presence of 4 M urea, and the fluorescence intensity decreased to about 90%. In the presence of 8 M urea, the fluorescence intensity decreased to 40% and the spectral maximum largely shifted to 356 nm. In the following experiments, fluorescence emission was monitored at 332 or 340 nm for *Ec*-IPMDH or *Tt*-IPMDH, respectively.

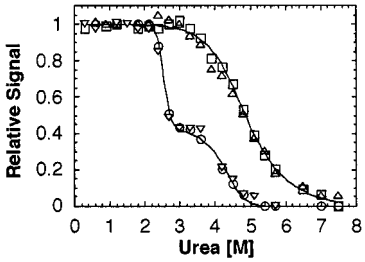

FIGURE 2: Unfolding of *Ec*-IPMDH and of *Tt*-IPMDH monitored by fluorescence and CD. Urea-induced equilibrium unfolding of 1.6 μM *Ec*-IPMDH and 1.6 μM *Tt*-IPMDH was monitored by CD at 222 nm (○, *Ec*-IPMDH; □, *Tt*-IPMDH) or by fluorescence emission at 332 (▽, *Ec*-IPMDH) or 340 nm (△, *Tt*-IPMDH) with excitation at 280 nm. *Ec*-IPMDH or *Tt*-IPMDH samples were incubated under the same conditions described in the legend of Figure 1. Solid lines represent curve fits to the fluorescence data.

Figure 2 shows the equilibrium unfolding of 1.6 μM *Ec*-IPMDH and 1.6 μM *Tt*-IPMDH monitored by CD at 222 nm and by intrinsic fluorescence emission. The relative change in the CD signal could almost be superimposed on the relative change in fluorescence intensity for the respective enzymes. The reduction in secondary structure monitored by CD and in tertiary structure monitored by fluorescence intensity of *Ec*-IPMDH and *Tt*-IPMDH appeared to be biphasic. The first phase of unfolding of *Ec*-IPMDH was a decrease in both signals between 2.2 and 2.8 M urea, and the second phase was a decrease observed between 3.5 and 5.5 M urea. The first phase of *Tt*-IPMDH unfolding was a slight decrease in the signals between 3.5 and 4.0 M urea, and the second phase was a decrease between 4.4 and 8.0 M urea. Though the biphasic characteristics of the unfolding curves of *Tt*-IPMDH were not as clear as those of *Ec*-IPMDH, there was reproducibly a small shoulder at around 4 M urea. These results suggest the presence of a stable intermediate in equilibrium with the native and the unfolded species, for each IPMDH. However, the intermediate of *Ec*-IPMDH lost its secondary and tertiary structure to a larger extent than did that of *Tt*-IPMDH.

Figure 3 shows the urea-induced unfolding of two different concentrations of *Ec*-IPMDH and *Tt*-IPMDH. As can be seen in Figure 3A, the first transition of the *Ec*-IPMDH unfolding was independent of protein concentration, whereas the midpoint of the second transition shifted to the right and the relative signal of this transition increased slightly as the IPMDH concentration was increased. This protein concentration dependence suggests that *Ec*-IPMDH dissociates during the second transition. In Figure 3B, the midpoint of the second transition of *Tt*-IPMDH shifted to a higher urea concentration when the IPMDH concentration was increased. Though the concentration dependence of the first transition of *Tt*-IPMDH was unclear because of the small amplitude of the fluorescence decrease, the relative intensities of fluorescence coincided with each other at the urea concentration of <3.5 M.

Enzymatic Activity and ANS Binding. Both the thermophilic and the mesophilic IPMDHs have two identical catalytic centers between two structural domains of each subunit, which are also shared between two subunits (*8*). They are therefore expected to be active only in the dimeric

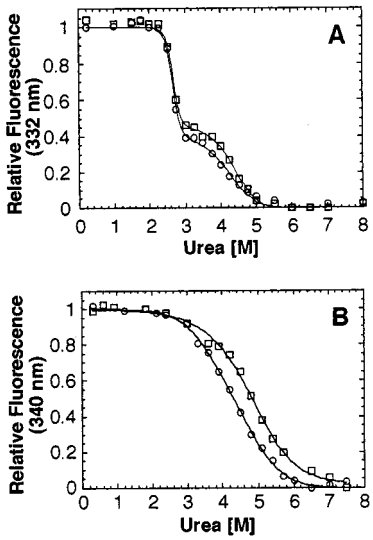

FIGURE 3: Protein concentration dependence of unfolding of *Ec*-IPMDH and *Tt*-IPMDH. Unfolding of *Ec*-IPMDH (A) or *Tt*-IPMDH (B) was monitored by fluorescence emission at 332 or 340 nm, respectively, with excitation at 280 nm. Protein concentrations were 2.96 μM (□) and 0.74 μM (○) for *Ec*-IPMDH and 1.64 μM (□) and 0.33 μM (○) for *Tt*-IPMDH. IPMDH samples were unfolded under the same conditions as described in the legend of Figure 1. Solid lines represent curve fits as described in Experimental Procedures.

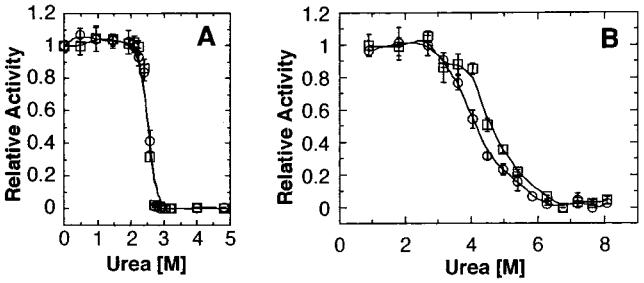

FIGURE 4: Enzymatic activity in the presence of urea. Equilibrium unfolding of *Ec*-IPMDH (A) and of *Tt*-IPMDH (B) was monitored by enzymatic activity. Protein concentrations 2.96 (□) and 0.74 μM (○) for *Ec*-IPMDH and 1.64 (□) and 0.33 μM (○) for *Tt*-IPMDH. IPMDH samples were unfolded under the same conditions as described in the legend of Figure 1 before the activity measurements. Error bars show the maximum and the minimum values of the repeated measurements. Catalytic activity was measured in the assay buffer containing the respective concentrations of urea as described in Experimental Procedures.

form with both domains intact. Panels A and B of Figure 4 show the loss of enzymatic activity of *Ec*-IPMDH and *Tt*-IPMDH, respectively. Figure 4A shows that the activity of *Ec*-IPMDH was lost between 2.2 and 2.8 M urea, which corresponds to the first transition monitored by fluorescence and CD. The midpoint of the unfolding was at about 2.6 M urea and was independent of the protein concentration. *Ec*-IPMDH lost its enzymatic activity in the first transition from the native to the intermediate state. The molecules in the intermediate state must be inactive. The protein concentration independence supports the idea that the first transition of *Ec*-IPMDH does not involve the dissociation of the dimer, and that the intermediate is still dimeric. The intermediate species of *Ec*-IPMDH do not have its enzymatic activity probably because the catalytic sites are disrupted prior to subunit dissociation. As shown in Figure 4B, the unfolding curve obtained from the loss of the enzyme activity of 1.6

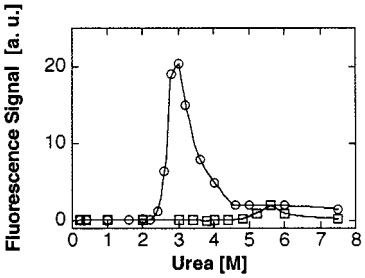

FIGURE 5: Enhancement of ANS fluorescence by denatured samples of *Ec*-IPMDH and *Tt*-IPMDH. *Ec*-IPMDH (0.33 μM) (○) and *Tt*-IPMDH (0.33 μM) (□) were unfolded by urea under the same conditions as described in the legend of Figure 1 and then incubated with a 50-fold molar excess of ANS for 60 min in the dark at 27 °C. ANS fluorescence was excited at 350 nm, and emission intensity was measured at 470 nm in the presence of IPMDH. The appropriate blank spectra of ANS were subtracted from the signal, and the resulting fluorescence enhancement (au, arbitrary units) was plotted.

μM *Tt*-IPMDH coincided roughly with that obtained from fluorescence and CD measurements. The midpoint of the second transition shifted to a lower urea concentration when the protein concentration was lowered. These observations suggest that the intermediates of *Tt*-IPMDH are still active and retain their dimeric structure and most of their tertiary structure.

The hydrophobic fluorescent dye ANS was used to probe the exposure of the hydrophobic region upon urea-induced unfolding of *Ec*-IPMDH and *Tt*-IPMDH (Figure 5). ANS increases its fluorescence quantum yield upon noncovalent binding to hydrophobic regions of proteins. The fluorescence emission spectra of ANS in the presence of native IPMDHs were similar to that of ANS in the buffer. A steep increase in ANS fluorescence enhancement was observed during the first transition of *Ec*-IPMDH (Figure 5), accompanied by a blue shift of ANS emission spectra (data not shown). After a sharp maximum, the degree of ANS fluorescence enhancement steeply decreased, preceding the second transition observed by protein fluorescence and CD. *Tt*-IPMDH showed no change of ANS fluorescence enhancement during the first transition, and only a small enhancement was observed during the second transition.

DISCUSSION

The equilibrium unfolding processes of *Ec*-IPMDH and *Tt*-IPMDH monitored by fluorescence and CD spectroscopy were biphasic. The simplest model that accounts for all the experimental observations is

$$N_2 \leftrightarrow I_2 \leftrightarrow D + D \qquad (1')$$

in which the protein is assumed to be in a native dimeric state (N_2), in a dimeric intermediate state (I_2), or unfolded subunits (D + D). However, the intermediates of *Ec*-IPMDH and *Tt*-IPMDH showed characteristics that differed between each other. At the first transition from the native state to the intermediate state, *Ec*-IPMDH lost more than 50% of its secondary and tertiary structure of the native state, accompanied by exposure of inner hydrophobic regions to the solvent. The amount of secondary and tertiary structure of the thermophilic enzyme only decreased to 90% of that of the native form in the first transition. The intermediate of

Table 1: Thermodynamic Parameters Obtained from Equilibrium Unfolding of *Tt*-IPMDH and *Ec*-IPMDH As Monitored by Fluorescence

protein	concentration (μM)	$\Delta G_1°$ (kcal/mol)[a]	$\Delta G_2°$ (kcal/mol)[a]	$\Delta G°$ (kcal/mol)[b]	m_1 (kcal mol^{-1} M^{-1})[a]	m_2 (kcal mol^{-1} M^{-1})[a]
Tt-IPMDH	0.33	4.51	16.3	(16.8)	1.20	1.41
Tt-IPMDH	1.6	4.52	18.4	(17.6)	1.35	1.60
Ec-IPMDH	0.74	14.7	17.7		5.56	2.22
Ec-IPMDH	3.0	15.9	19.0		5.99	2.74

[a] Free energy changes $\Delta G_1°$ and $\Delta G_2°$ and cooperativity indices m_1 and m_2 were obtained from a curve fit based on a three-state model ($N_2 \leftrightarrow I_2 \leftrightarrow D + D$). [b] Free energy change $\Delta G°$ was obtained from a curve fit based on a simple two-state model ($N_2 \leftrightarrow D + D$).

the mesophilic enzyme was enzymatically inactive, whereas the thermophilic one remained active.

The presence of the intermediate state in *Tt*-IPMDH was not as obvious as in *Ec*-IPMDH. However, a small shoulder in the unfolding curve was reproducible. Thus, we treated the unfolding process of *Tt*-IPMDH on the basis of the three-state model. The intermediate of *Tt*-IPMDH was, however, still enzymatically active and showed no ANS binding ability. So the transition from the native to the intermediate state must be a very small isomerization in *Tt*-IPMDH.

We have previously investigated the stability of oligomeric structures of *Ec*-IPMDH and *Tt*-IPMDH by urea−polyacrylamide gel electrophoresis at 30 °C (*3*). We have shown that *Ec*-IPMDH dissociated completely while *Tt*-IPMDH was stable as a dimer in 6 M urea. In 4 M urea, the fraction of *Ec*-IPMDH in monomeric form appeared to be almost the same as the fraction in dimeric form. In the present experiment, we showed that *Ec*-IPMDH dissociated from the intermediate form to the unfolded monomeric form at around 4.2 M urea and that *Tt*-IPMDH dissociated at around 5.3 M urea. With regard to *Ec*-IPMDH, the current results were consistent with the previous results obtained by electrophoresis. The dimeric form of *Tt*-IPMDH seemed to be less stable in 6 M urea in this report, which is probably because the duration of the urea treatment was longer than in the previous experiment (15 min).

Though most dimeric proteins unfold directly into the monomeric unfolded state in equilibrium (*9*−*11*), a significant number of dimeric proteins are reported to unfold via monomeric intermediates before the total unfolding (*12*−*19*). Only a few are reported to unfold via an intermediate state with dimeric structure (*7*, *20*, *21*). Clark et al. (*7*) have reported a dimeric intermediate of bacterial luciferase. The enzyme in the dimeric intermediate state did not have catalytic activity but retained about 50% of its secondary structure. Glutathione transferase B1-1 showed multiphasic denaturation with a dimeric intermediate state without catalytic activity, which retained secondary and tertiary structure (*20*). Mei et al. (*21*) have reported a dimeric intermediate of ascorbate oxidase, which retained the secondary structure of the native protein but lost its tertiary structure as well as its catalytic activity.

The intermediate state of *Ec*-IPMDH is similar to that of bacterial luciferase in the sense that both proteins retain about half of their secondary structure. The intermediate of *Tt*-IPMDH retained most of its secondary and tertiary structure and was similar to that reported for glutathione transferase B1-1. However, glutathione transferase B1-1 shows no catalytic activity in the intermediate state.

We have previously investigated the heat denaturation process of chimeric IPMDH, which consists of parts of *Tt*-IPMDH and *Bacillus subtilis* IPMDH, with differential scanning calorimetry and CD (*22*). The chimeric IPMDH exhibited a three-state denaturation process. The intermediate state retained about half of the secondary and tertiary structure. Both the first and the second transitions of the heat denaturation process were accompanied by an endothermal process. The biphasic denaturation was interpreted as independent denaturation of two domains; the first domain containing both N and C termini denatured first, and the second domain which contains the subunit−subunit interface denatured next. Sequential unfolding of individual conformational domains has been reported also for some oligomeric proteins (*7*, *16*, *23*). The equilibrium unfolding of *Ec*-IPMDH may be such sequential unfolding of two domains.

Alternatively, the intermediate state of *Ec*-IPMDH may be in the molten globule-like state as reported for other dimeric proteins (*12*, *21*). However, the partially unfolded intermediate of *Ec*-IPMDH appeared to be still dimeric, which indicates that the second domain involving the subunit interaction remains folded after the first unfolding transition. Furthermore, the coincidence of unfolding curves measured by fluorescence and by CD was consistent with a domain-unfolded intermediate, rather than with a molten globule-like intermediate, because the molten globule usually retains a large portion of secondary structure and little tertiary structure (*24*). The high capacity for ANS binding in the intermediate state of *Ec*-IPMDH may be attributed to the exposure of a hydrophobic domain−domain interface upon the unfolding of the first domain.

The free energy differences between folded, intermediate, and unfolded states were calculated using the three-state model (eq 1) as described in Experimental Procedures (Table 1). The free energy differences between the folded and the intermediate states, $\Delta G_1°$, and between the intermediate and the unfolded states, $\Delta G_2°$, were about 14.7 and 17.7 kcal/mol, respectively, for *Ec*-IPMDH. $\Delta G_1°$ and $\Delta G_2°$ of *Tt*-IPMDH were 4.51 and 16.3 kcal/mol, respectively. These values are comparable to those reported for other dimeric proteins (*7*, *9*, *14*, *19*). It should be noted that $\Delta G_1°$ and $\Delta G_2°$ of *Tt*-IPMDH are not larger than those of *Ec*-IPMDH. The free energy difference between the unfolded state and the folded state of *Tt*-IPMDH based on the simple two-state model was also calculated and presented in Table 1. The free energy difference of total unfolding became even smaller than that obtained from the three-state model. The experiments for determining the temperature dependence of the free energy difference of the unfolding process of IPMDHs are in progress. The $\Delta G°$ values of *Tt*-IPMDH that were smaller than those of *Ec*-IPMDH were observed at temperatures of <40 °C in the preliminary experiments, and the results will be published elsewhere. The higher thermal stability of *Tt*-IPMDH is represented by the activity retained in the intermediate state. In other words, the intermediate

state of *Tt*-IPMDH retains the structural integrity to support the enzymatic activity in contrast to *Ec*-IPMDH. The fluctuation of the local structure does not seriously affect the active sites in the intermediate state of *Tt*-IPMDH. Alternatively, the fluctuation of the structure may be restored during the binding process of substrate and/or of cofactors of the catalytic reaction. One or more of the loops (from P110 to E120 and/or from G71 to P86), which have relatively high *B*-factors in crystallographic analysis, may be partially unfolded.

The relative structural integrity of the *Tt*-IPMDH intermediate is provided by the increase of the interaction of the moiety which unfolded prior to the unfolding of the whole molecular structure in *Ec*-IPMDH, probably the first domain containing C and N termini. We have previously studied the increase of the thermal stability of IPMDH from *B. subtilis* using an evolutionary molecular engineering technique (*25*). We found that the mutations in the first domain were effective in increasing the thermal stability of *B. subtilis* IPMDH. The present results provide further support for the previous finding that the larger interaction at the moiety which unfolds first is effective in improving the stability of multidomain proteins.

We have treated and discussed the unfolding process of *Tt*-IPMDH in the three-state model with the active intermediate so far. However, the relative change in fluorescence and CD signals in the first phase was not so large and the intermediate state showed catalytic activity. Accordingly, the intermediate may be simply regarded as an alternative form of native molecules. Moreover, the unfolding process could be analyzed in the two-state model ($N_2 \Leftrightarrow D + D$). However, it should be noted that the discussion regarding the relative thermal stability of *Tt*-IPMDH still holds true in these alternative models. In these models, the interaction within the portion unfolded first in *Ec*-IPMDH was increased and the intermediate has disappeared to show the cooperative unfolding from N_2 to the 2D state directly.

REFERENCES

1. Yamada, T., Akutsu, N., Miyazaki, K., Kakinuma, K., Yoshida, M., and Oshima, T. (1990) *J. Biochem. 108*, 449−456.
2. Imada, K., Sato, M., Tanaka, N., Katsube, Y., Matsuura, Y., and Oshima, T. (1991) *J. Mol. Biol. 222*, 725−738.
3. Kirino, H., Aoki, M., Aoshima, M., Hayashi, Y., Ohba, M., Yamagishi, A., Wakagi, T., and Oshima, T. (1994) *Eur. J. Biochem. 220*, 275−281.
4. Wallon, G., Kirino-Kagawa, H., Yamagishi, A., Yamamoto, K., Lovett, S. T., Petsko, G. A., and Oshima, T. (1996) *Biochim. Biophys. Acta 1337*, 105−112.
5. Wallon, G., Kryger, G., Lovett, S. T., Oshima, T., Ringe, D., and Petsko, A. (1997) *J. Mol. Biol. 266*, 1016−1031.
6. Pace, C. N., Shirley, B. A., and Thomson, J. A. (1989) in *Protein Structure, A Practical Approach* (Creighton, T. E., Ed.) pp 311−330, IRL Press, New York.
7. Clark, A. C., Sinclair, J. F., and Baldwin, T. O. (1993) *J. Biol. Chem. 268*, 10773−10779.
8. Kadono, S., Sakurai, M., Moriyama, H., Sato, M., Hayashi, Y., Oshima, T., and Tanaka, N. (1995) *J. Biochem. 118*, 745−752.
9. Neet, K. E., and Timm, D. E. (1994) *Protein Sci. 3*, 2167−2174.
10. Rietveld, A., and Ferreira, S. (1998) *Biochemistry 37*, 933−937.
11. Wallace, L., Sluis-Cremer, N., and Dirr, H. (1998) *Biochemistry 37*, 5320−5328.
12. Herold, M., and Kirshner, K. (1990) *Biochemistry 29*, 1907−1913.
13. Aceto, A., Caccuri, A., Sacchetta, P., Bucciarelli, T., Dragani, B., Rosato, N., Federici, G., and Di Ilio, C. (1992) *Biochem. J. 285*, 241−245.
14. Cheng, X., Gonzalez, M. L., and Lee, J. C. (1993) *Biochemistry 32*, 8130−8139.
15. Timm, D., Haseth, P., and Neet, K. (1994) *Biochemistry 33*, 4667−4676.
16. Gross, M., Lustig, A., Wallimann, T., and Furter, R. (1995) *Biochemistry 34*, 10350−10357.
17. Abu-Soud, H., Loftus, M., and Stuehr, D. (1995) *Biochemistry 34*, 11167−11175.
18. Couthon, F., Clottes, E., Ebel, C., and Vial, C. (1995) *Eur. J. Biochem. 234*, 160−170.
19. Malecki, J., and Wasylewski, Z. (1997) *Eur. J. Biochem. 243*, 660−669.
20. Sacchetta, P., Aceto, A., Bucciarelli, T., Dragani, B., Santarone, S., Allocati, N., and Di Ilio, C. (1993) *Eur. J. Biochem. 215*, 741−745.
21. Mei, G., Di Venere, A., Buganza, M., Vecchini, P., Rosato, N., and Finazzi-Agro', A. (1997) *Biochemistry 36*, 10917−10922.
22. Hayashi-Iwasaki, Y., Numata, K., Yamagishi, A., Yutani, K., Sakurai, M., Tanaka, N., and Oshima, T. (1996) *Protein Sci. 5*, 511−516.
23. Le Bras, G., Techner, W., Deville-Bonne, D., and Garel, J. (1989) *Biochemistry 28*, 6836−6841.
24. Kuwajima, K. (1989) *Proteins: Struct., Funct., Genet. 6*, 87−103.
25. Akanuma, S., Yamagishi, A., Tanaka, N., and Oshima, T. (1998) *Protein Sci. 7*, 698−705.

BI982380V